Energy of the amplitude mode in the bicubic antiferromagnet: Series expansion results

J. Oitmaa
School of Physics, The University of New South Wales, Sydney NSW 2052, Australia

(Received 4 March 2018; published 23 May 2018)

Series expansion methods are used to study the quantum critical behavior of the bicubic spin-1/2 antiferromagnet. Excitation energies are computed throughout the Brillouin zone, for both the Néel and dimer phases. We compute the energy of the amplitude/Higgs mode and show that it becomes degenerate with the magnon modes at the quantum critical point, as expected on general symmetry grounds.

DOI: 10.1103/PhysRevB.97.174421

I. INTRODUCTION

Experimental and theoretical studies of elementary excitations in quantum antiferromagnets have, until recently, focused on one-magnon modes—transverse fluctuations of the spins about the spontaneously selected ordering direction.

However, it was noted already some years ago [1] that a mode involving longitudinal spin fluctuations is also present, and may play a significant role in physical properties, particularly near a quantum critical point. In recent years many papers have discussed this "amplitude" or "Higgs" mode [2–6], from different perspectives and using different techniques. Moreover, there are experimental observations of this mode in at least two different materials [7–10].

In studies of quantum phase transitions, the spin-1/2 Heisenberg antiferromagnet on a square lattice bilayer has played a major role. It is well known that this system has an O(3) quantum critical point (QCP) at $g = 2.522\ldots$ [11] (where g is the ratio of interlayer versus intralayer coupling), between an ordered Néel ground state and a dimerized nonmagnetic ground state with singlet dimers on the rungs between the planes. Using series expansions, we were able to identify the amplitude mode in this system [12], to show that it becomes gapless at the QCP, and thus restores the symmetry between the number of soft modes in each phase at the QCP. More recently, the bilayer system has been generalized to three spatial dimensions, as a pair of coupled simple-cubic lattices—the "bicubic" lattice [5,6]. Using quantum Monte Carlo (QMC) simulations, these authors were able to locate the QCP, with remarkable precision, at $g = 4.8370\ldots$. They were also able to identify the amplitude mode, and to show that its energy was in accord with general field theory predictions [13]. The approach used in each of these papers was to compute the dynamical spin structure factor $S(\mathbf{k},\omega)$ and a suitably defined dimer structure factor $D(\mathbf{k},\omega)$ (denoted by S_B in Ref. [5]). The amplitude/Higgs mode is seen as a rather broad peak, which sharpens and softens as the QCP is approached.

The present work investigates the bicubic model using series expansions at zero temperature. It thus represents an extension of the work of Ref. [12] to the three-dimensional (3D) bicubic system. Although this approach cannot match the high precision of the QMC results, it does have the advantage that the energies of excitations, magnon, and amplitude modes in the ordered phase and triplon modes in the dimer phase can be computed directly throughout the Brillouin zone as full dispersion curves.

The organization of the paper is as follows: in Sec. II we describe the method used for our calculations, and present a summary of results. In Sec. III we discuss the results for excitations in more detail, and show plots of the dispersion curves for various values of the coupling g. In the final section we summarize and draw conclusions.

II. SERIES EXPANSIONS

The bicubic lattice, shown in Fig. 1, consists of two simple-cubic lattices, which we refer to as sublattices A and B, with $S = 1/2$ spins at the vertices of each sublattice. Each spin is coupled to its six nearest neighbors on its own sublattice with an isotropic Heisenberg exchange interaction of strength J. In addition adjacent A and B spins are coupled by an exchange J_d.

Thus the Hamiltonian of our model is

$$H = J \sum_{\langle ij \rangle}^{(1)} \mathbf{S_i} \cdot \mathbf{S_j} + J_d \sum_{\langle il \rangle}^{(2)} \mathbf{S_i} \cdot \mathbf{S_l}, \qquad (1)$$

where the sums are over bonds within and between sublattices, respectively. All couplings are taken to be antiferromagnetic.

As noted above, this is a natural generalization to three spatial dimensions of the much studied bilayer system. For $J_d = 0$ we have two decoupled simple-cubic lattices, each of which will exhibit Néel order at low temperatures, up to a critical temperature T_N. This phase will persist for nonzero J_d, up to a critical value $g_c = (J_d/J)_c$, at which point T_N will fall to zero and the system will enter a nonmagnetic dimer phase with short-range correlations.

We use long perturbative series expansions to probe the bulk properties of each phase at $T = 0$, as well as the energy spectra of elementary excitations. High-temperature series expansions could also be used to compute thermodynamic properties in the paramagnetic phase and to find the variation of T_N with g, but we do not report on this here.

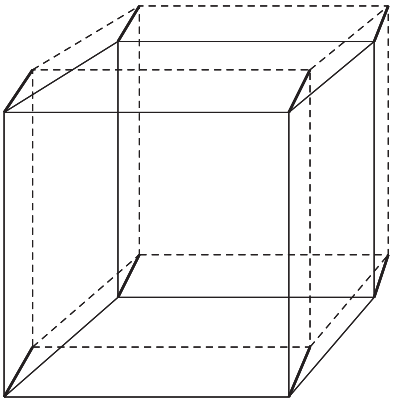

FIG. 1. Structure of the bicubic lattice. Thin solid and dashed lines represent the two simple-cubic lattices. Thick solid lines represent the J_d bonds.

A. Dimer phase expansions

To compute series in the dimer phase we separate the Hamiltonian as $H = H_0 + \lambda V$, where H_0 represents the dimer terms (for convenience we set $J_d = 1$ here, and V represents the interactions within each sublattice). The expansion parameter is then $\lambda = J/J_d = 1/g$. The unperturbed ground state is a simple product state with singlet dimers $|s\rangle = 1/\sqrt{2}[|+-\rangle - |-+\rangle]$ on each J_d bond, and the V term allows this to evolve into the true ground state. The ground-state energy E_0 can be computed as a power series in λ,

$$E_0/NJ_d = -3/8 + \sum_{r=1}^{\infty} e_r \lambda^r, \tag{2}$$

where the number of spins is $2N$, and the e_r are numerical coefficients.

We use the "linked-cluster" method [14,15] to compute this series, to order λ^{10}. This method is well established, and has been used successfully to study the bilayer system [16]. The reader is referred to the expositions [14,15] for technical details. The present calculation requires 1050 distinct connected clusters with ten or fewer sites.

In Table I we give the values of the series coefficients to 12 significant figures. In principle they could be computed as exact rational fractions but, for our purposes, this is unnecessary.

TABLE I. Coefficients of the dimer expansion for E_0.

0	$-0.375\,000\,000\,000D+00$
1	$0.000\,000\,000\,000D+00$
2	$-0.562\,500\,000\,000D+00$
3	$-0.281\,250\,000\,000D+00$
4	$-0.386\,718\,750\,000D+00$
5	$0.123\,046\,875\,000D+00$
6	$-0.222\,802\,734\,375D+01$
7	$-0.303\,469\,848\,633D+01$
8	$-0.210\,607\,910\,156D+02$
9	$-0.232\,059\,102\,058D+02$
10	$-0.203\,792\,628\,050D+03$

To evaluate the energy as a function of g we use Padé approximant methods [15]. This series is, in fact, rapidly convergent, reflecting the short range of correlations in the dimer phase, and even a naive sum of the available terms suffices, except close to g_c.

However, our main interest in the present work is the excitation spectrum. In the unperturbed system an excitation consists of exciting a single dimer from its singlet $S = 0$ state to one of the three degenerate $S = 1$ triplet states, which costs an energy of J_d. The V terms will then allow this excitation to propagate through the dimer system, resulting in a band of triply degenerate "triplon" excitations, with an energy spectrum $\epsilon_{\text{triplon}}(\mathbf{k})$. Pioneering work by Gelfand [17] showed how excitation spectra could also be calculated via a linked-cluster method, and this approach is also well established [15].

The excitation energy is expressed in the form

$$\epsilon(\mathbf{k}) = \sum_{\mathbf{r}} \gamma_{\mathbf{k}}(\mathbf{r})\mathbf{t}(\mathbf{r}), \tag{3}$$

where the sum is over hopping vectors $\mathbf{r}$ on the lattice, the $t(\mathbf{r})$ are transition matrix elements, which are computed as power series in λ, and the $\gamma_{\mathbf{k}}(\mathbf{r})$ are structure factors,

$$\gamma_{\mathbf{k}}(\mathbf{r}) = [\cos(k_x x)\cos(k_y y)\cos(k_z z) + \text{permutations}]/6. \tag{4}$$

Our calculation, to eighth order, involves a total of 29 931 distinct clusters with all space types, with nine or fewer sites.

A figure showing the triplon spectrum (Fig. 3) and a discussion are given in the following section.

B. Néel phase expansions

In the small g Néel phase we use a different separation $H = H_0 + \lambda V$, with H_0 consisting of the diagonal $S_i^z S_j^z$ terms. This is an "Ising expansion," where the unperturbed Hamiltonian exhibits antiferromagnetic Néel order, but without quantum fluctuations, and the perturbation V restores these fluctuations to recover the full quantum Hamiltonian. For technical reasons it is convenient to introduce a transformation $(S^x, S^y, S^z) \rightarrow (S^x, -S^y, -S^z)$ on alternate sites, to give a uniform fully aligned unperturbed ground state. Then

$$H_0 = -J \sum_{\langle ij \rangle}^{(1)} S_i^z S_j^z - J_d \sum_{\langle il \rangle}^{(2)} S_i^z S_l^z \tag{5}$$

and

$$V = \frac{1}{2} J \sum_{\langle ij \rangle}^{(1)} (S_i^+ S_j^+ + S_i^- S_j^-) + \frac{1}{2} J_d \sum_{\langle il \rangle}^{(2)} (S_i^+ S_l^+ + S_i^- S_l^-). \tag{6}$$

Again we use linked cluster expansions to obtain series for bulk ground-state properties and excitation spectra, as power series in λ. In this case a separate calculation is required for each parameter J_d (we set $J = 1$ for convenience), and the series need to be evaluated at $\lambda = 1$ to regain the isotropic Hamiltonian. Because of this we do not present series coefficients, but they are available on request.

The magnon energies in the Néel phase are computed by starting from a manifold of unperturbed states with a single flipped spin. The perturbation V then allows these states to

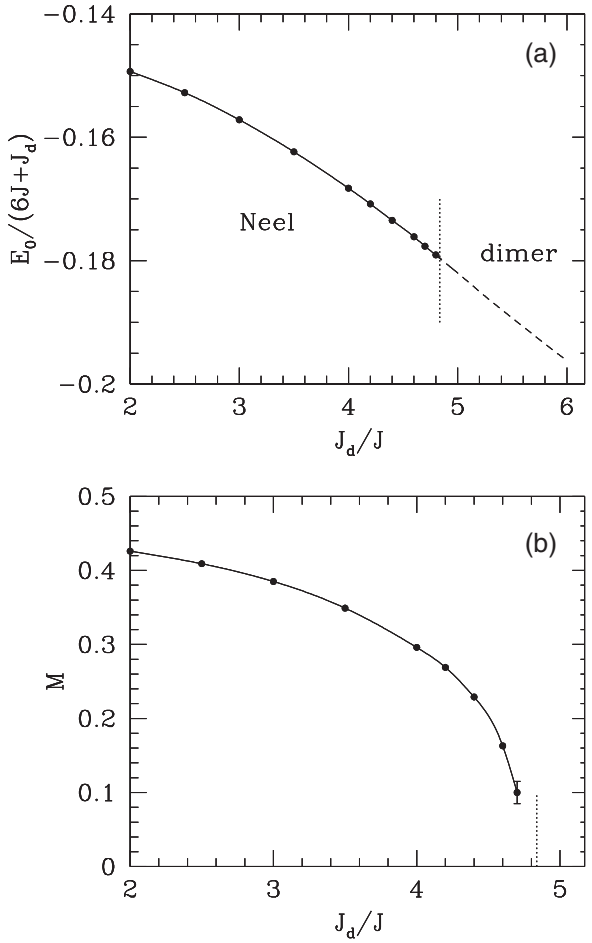

FIG. 2. Ground-state energy in the Néel and dimer phases (a), and Néel phase order parameter (b), from series expansions. Uncertainties are no larger than the size of points. The lines are a guide for the eye. The thin vertical lines indicate the position of the QCP.

mix and propagate, leading to an "effective Hamiltonian" matrix for each cluster. The transition amplitudes for the bulk lattice are then obtained from these matrix elements, and the magnon energies are finally given by an expression similar to (3). Because of the reflection symmetry between the two sublattices, the spectrum has two branches: one which is of even parity under sublattice interchange, and the other of odd parity. These can be described in terms of a wave-vector component $k_p = 0,\pi$ in a fourth spatial dimension. The two branches are related by

$$\epsilon(k_x,k_y,k_z,0) = \epsilon(\pi - k_x,\pi - k_y,\pi - k_z,\pi). \qquad (7)$$

A similar feature occurs in the bilayer system [16].

Finally we consider the amplitude mode. This can be regarded as a bound state of two magnons, in the sense that it appears as a pole in the two-particle Green's function [1]. Hence the manifold of unperturbed states consists of pairs of flipped spins on the J_d bonds. There is a technical complication since the two-magnon sector has the same total spin as the ground-state sector. This requires that the effective Hamiltonian matrix for each cluster be fully block diagonalized, using the so-called "multiblock method" [18], which is computationally more demanding. Our calculation, to order λ^8,

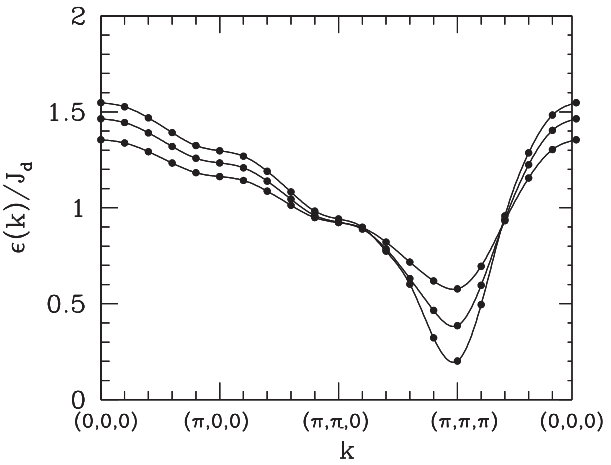

FIG. 3. Dimer phase triplon excitation energies along symmetry lines in the Brillouin zone, for three value of the coupling constant g, as $g = 6.0,5.5,5.0$ [from top to bottom at (π,π,π)].

requires a total of 1 122 545 distinct clusters with up to nine sites.

III. RESULTS AND DISCUSSION

Although our main interest is in the excitations, it seems worthwhile to display some results for the bulk energy and order parameter. Figure 2(a) gives the ground-state energy as a function of g in both the Néel and dimer phases. The two curves meet smoothly in the vicinity $g \sim 5.0$, but it is not possible to determine g_c from this plot with any degree of precision. Figure 2(b) shows the Néel phase magnetization, which is clearly vanishing as the QCP is approached. This series becomes rather irregular near the QCP, with quite large error bars. However, the behavior is as expected. It is worth pointing out here that error bars, where shown in this and subsequent figures are "confidence limits" based on consistency between different Padé approximants, and not true statistical errors.

In the previous section we described how the excitation spectra in both the dimer phase and the Néel phase can be computed. Here we will present our results, largely in the form of figures, and discuss their significant features.

In Fig. 3 we show the energy of triplon excitations, along a path in the cubic Brillouin zone, for three different values of g.

As is evident, the excitation at $\mathbf{k} = (\pi,\pi,\pi)$ softens as the critical point is approached, as expected. To investigate this more closely, we obtain a series for the energy gap Δ and analyze this directly. The series coefficients are given in Table II.

The series for the triplon gap can be summed directly using Padé approximants. The resulting plot shows the gap vanishing at a value $g_c = 4.85 \pm 0.05$. It is also possible to estimate g_c by identifying the physical singularity in the series from Dlog Padé approximants. The highest-order central approximants show a singularity at $1/g = 0.208 \pm 0.001$ with an exponent of $\sim$0.6, from which one might conclude that $g_c = 4.81 \pm 0.02$. However, since this system is at the upper space-time critical dimension for an O(3) critical point, we expect mean-

TABLE II. Coefficients of the energy gap series in the dimer phase.

0	$0.100\,000\,000\,000D+01$
1	$-0.300\,000\,000\,000D+01$
2	$-0.150\,000\,000\,000D+01$
3	$-0.825\,000\,000\,000D+01$
4	$-0.206\,350\,000\,000D+02$
5	$-0.623\,203\,125\,000D+02$
6	$-0.196\,127\,929\,688D+03$
7	$-0.821\,838\,867\,223D+03$
8	$-0.305\,614\,173\,882D+04$

field behavior with logarithmic corrections, of the form

$$\Delta \sim \left(\frac{g}{g_c}-1\right)^{1/2} \ln^{-\overline{\nu}}\left(\frac{g}{g_c}-1\right). \tag{8}$$

The QMC work [5,6] has shown that the logarithm term is significant in the analysis, with an estimated $\overline{\nu} \sim 0.23$. We also find this in a more detailed analysis of the series, since the data cannot be well fitted by a simple square-root form, although we have not attempted to compute the logarithm term. However, we can improve upon our raw Padé analysis by evaluating approximants to the series for $(1-\frac{g_c}{g})^{-1/2}\Delta$, where we have used the QMC value $g_c = 4.837$. The data in Fig. 4 have been obtained in this way, and the points are in excellent agreement with the QMC results [5,6].

We now turn to the excitations in the Néel phase. In Fig. 5(a) we show the energies of even parity one-magnon states along a path through the Brillouin zone, for three values of the parameter J_d. The results are quite well converged, except near the Γ point (0,0,0). These are the Goldstone modes where $\epsilon(\mathbf{k}) = 0$, but it is difficult to reproduce this using short series, as has been noted many times in the past. An interesting feature is the appearance of a dip at (π,π,π) for small J_d, which disappears for larger J_d. We have no physical explanation for this. Otherwise the curves are relatively featureless. In Fig. 5(b) we show the dispersion curves for the odd parity modes. While these are related to the even parity modes via Eq. (7), the figure allows us to see clearly that the odd parity magnon and triplon become degenerate at the QCP.

In Fig. 6 we show the energies of the amplitude/Higgs mode along the same path in the Brillouin zone, for values $J_d = 3.0, 4.75$. A number of points can be made. (1) Throughout most of the Brillouin zone, for these values of J_d, the amplitude mode appears to be stable, reflected by the regularity of the series and the absence of error bars. (2) Close to the Γ point (0,0,0) the series become erratic, particularly for $J_d = 3.0$, less so for $J_d = 4.75$ which is close to the QCP at $J_d = 4.837$. We surmise that this is an indication that the amplitude mode is not stable here. (3) For a smaller value, $J_d = 2.0$, the series are highly erratic throughout the Brillouin zone (not shown in Fig. 6). This would suggest that the amplitude mode becomes less stable, the further we are from the QCP. This is fully in accord with the QMC results [5,6]. (4) Comparing the curves for $J_d = 3.0$ in Figs. 5(a) and 6 shows that the amplitude mode has a significantly higher energy than the one-magnon mode. This is again as expected. (5) The curves for $J_d = 4.75$ in Figs. 5 and 6 are seen to be very close to each other. This reflects the expectation that at the QCP the amplitude mode becomes degenerate with the magnons, as the SU(2) symmetry is restored at the QCP.

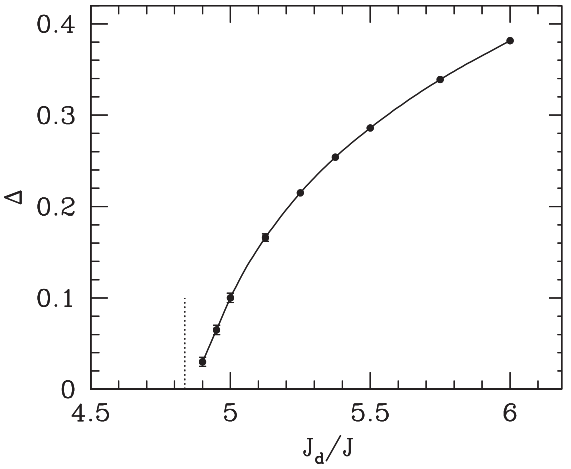

FIG. 4. Dimer phase energy gap at (π,π,π) vs g. The points are results of our analysis, with estimated errors no larger than the points. The line is a guide for the eye.

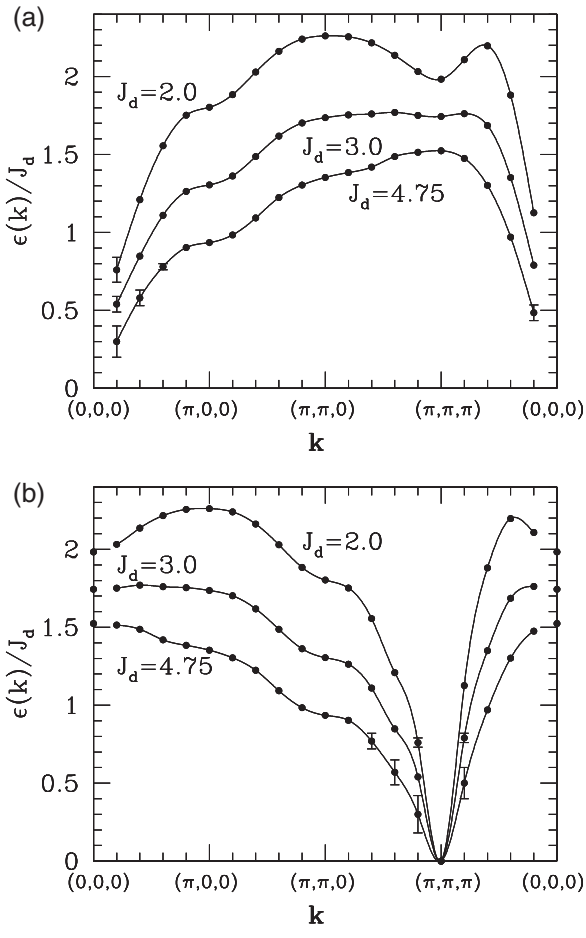

FIG. 5. Excitation energies for even parity one-magnon modes (a) and odd parity one-magnon modes (b), for a path through the Brillouin zone, for three values of J_d, as shown. The lines are guides for the eye.

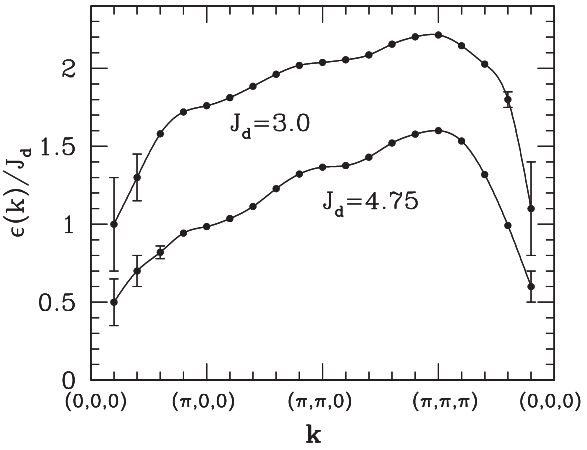

FIG. 6. Energy of the amplitude/Higgs mode along a path through the Brillouin zone, for two values of J_d as indicated.

IV. CONCLUSIONS

We have used series expansion methods to investigate the properties of a spin $S = 1/2$ "bicubic" Heisenberg antiferromagnet, formed by coupling two simple-cubic lattices. Recent quantum Monte Carlo studies of this system [5,6] have confirmed the existence of a quantum critical point with classical critical exponents, but with significant logarithmic corrections. The QMC work has also found a clear signature of the expected amplitude/Higgs mode as a broad low amplitude peak in the magnetic structure factor at the ordering wave vector, which sharpens and moves to lower energy as the QCP is approached.

The present work provides an independent study of this model, using a different method. Our results are in full agreement with the QMC work, as far as the location and nature of the QCP are concerned. In addition, the series method allows us to compute complete dispersion curves for excitations throughout the Brillouin zone, which the QMC approach is not naturally suited to do. We have been able, thus, to compute both magnon and amplitude mode energies in the ordered phase.

Previous identification of the amplitude mode in this model considered only the ordering wave vector, where the mode appears to be heavily overdamped and only sharpens close to the QCP. Our results suggest that the mode is, in general, sharper at other wave vectors in the Brillouin zone. We conjecture that the poor convergence of the series is a signature of instability in the mode, although this is a heuristic argument only.

Our results are consistent with a scenario in which the amplitude mode is not a well defined excitation far from the QCP, but becomes more stable as the QCP is approached and becomes degenerate with the magnon modes over the whole Brillouin zone at the QCP. Thus the amplitude and the magnon modes form a spin-1 multiplet at the QCP, in accord with the restoration of SU(2) symmetry.

ACKNOWLEDGMENTS

We are grateful for computing resources provided by the Australian Partnership for Advanced Computing (APAC) National Facility. We also thank O. Sushkov for valuable discussions.

[1] A. V. Chubukov and D. K. Morr, Phys. Rev. B **52**, 3521 (1995).
[2] S. Gazit, D. Podolsky, and A. Auerbach, Phys. Rev. Lett. **110**, 140401 (2013).
[3] D. Pekker and C. M. Varma, Annu. Rev. Condens. Matter Phys. **6**, 269 (2015).
[4] H. D. Scammell and O. P. Sushkov, Phys. Rev. B **92**, 220401(R) (2015).
[5] M. Löhofer and S. Wessel, Phys. Rev. Lett. **118**, 147206 (2017).
[6] Y. Q. Qin, B. Normand, A. W. Sandvik, and Z. Y. Meng, Phys. Rev. Lett. **118**, 147207 (2017).
[7] Ch. Rüegg, B. Normand, M. Matsumoto, A. Furrer, D. F. McMorrow, K. W. Krämer, H. U. Güdel, S. N. Gvasaliya, H. Mutka, and M. Boehm, Phys. Rev. Lett. **100**, 205701 (2008).
[8] P. Merchant, B. Normand, K. W. Krämer, M. Boehm, D. F. McMorrow, and Ch. Rüegg, Nat. Phys. **10**, 373 (2014).
[9] A. Jain, M. Krautloher, J. Porras, G. H. Ryu, D. P. Chen, D. L. Abernathy, J. T. Park, A. Ivanov, J. Chaloupka, G. Khaliullin, B. Keimer, and B. J. KIm, Nat. Phys. **13**, 633 (2017).
[10] S.-M. Souliou, J. Chaloupka, G. Khaliullin, G. Ryu, A. Jain, B. J. Kim, M. Le Tacon, and B. Keimer, Phys. Rev. Lett. **119**, 067201 (2017).
[11] L. Wang, K. S. D. Beach, and A. W. Sandvik, Phys. Rev. B **73**, 014431 (2006).
[12] C. J. Hamer, J. Oitmaa, and Z. Weihong, Phys. Rev. B **85**, 014432 (2012).
[13] H. D. Scammell, Y. Kharkov, Y. Q. Qin, Z. Y. Meng, B. Normand, and O. P. Sushkov, Phys. Rev. B **96**, 174414 (2017).
[14] M. P. Gelfand and R. R. P. Singh, Adv. Phys. **49**, 92 (2000).
[15] J. Oitmaa, C. J. Hamer, and W. Zheng, *Series Expansion Methods for Strongly Interacting Lattice Models* (Cambridge University Press, Cambridge, England, 2006).
[16] Z. Weihong, Phys. Rev. B **55**, 12267 (1997).
[17] M. P. Gelfand, Solid State Commun. **98**, 11 (1996).
[18] W. Zheng, C. J. Hamer, R. R. P. Singh, S. Trebst, and H. Monien, Phys. Rev. B **63**, 144410 (2001).